Available online at www.sciencedirect.com
SCIENCE DIRECT
Microporous and Mesoporous Materials 90 (2006) 188–197
MICROPOROUS AND MESOPOROUS MATERIALS
www.elsevier.com/locate/micromeso

Study of Mn incorporation into SAPO framework: Synthesis, characterization and catalysis in chloromethane conversion to light olefins

Yingxu Wei [a,b], Yanli He [a], Dazhi Zhang [a], Lei Xu [a], Shuanghe Meng [a], Zhongmin Liu [a,1], Bao-Lian Su [b,*]

[a] *Natural Gas Utilization and Applied Catalysis Laboratory, Dalian Institute of Chemical Physics, Chinese Academy of Sciences, P.O. Box 110, Dalian 116023, PR China*

[b] *Laboratoire de Chimie des Matériaux Inorganiques, ISIS, The University of Namur (FUNDP), 61 rue de Bruxelles, B-5000 Namur, Belgium*

Received 25 August 2005; received in revised form 21 October 2005; accepted 25 October 2005
Available online 15 December 2005

Dedicated to the late Denise Barthomeuf, George Kokotailo and Sergey P. Zhdanov in appreciation of their outstanding contributions to zeolite science

Abstract

MnAPSO-34 molecular sieve has been synthesized with triethylamine as the template, characterized with XRD, XRF, ^{31}P, ^{27}Al and ^{29}Si NMR and FT-IR techniques and compared with SAPO-34. The template decomposition and removal have been investigated with TG–DTG–DSC coupled with mass spectrometer. Mn incorporation generates a negligible difference on the chemical shift in ^{31}P and ^{27}Al MAS NMR, while an effect on the intensity of resonance peaks is revealed. ^{29}Si MAS NMR study has demonstrated that Mn incorporation favors the Si island formation, which may give rise to the stronger acidic sites. The thermal analysis (TG–DSC) on template removal in a diluted oxygen atmosphere, leading to the formation of CO_2, NO and H_2O, showed, besides a low temperature endothermic weight loss due to the desorption of water, two weight losses (200–400 and 400–600 °C) for SAPO-34 and MnAPSO-34, suggesting two different chemical location environments of template molecules in these two molecular sieves. The quantity of template removed at higher temperature range is much higher in MnAPSO-34, indicating stronger template–framework interaction and stronger acidity after calcination. The acid difference caused by Mn incorporation has also been evidenced by ammonia adsorption evaluated by FT-IR. Chloromethane transformation was carried out over MnAPSO-34 and SAPO-34 and the catalytic performance showed that both molecular sieves are very active and selective catalyst for light olefins production. MnAPSO-34 demonstrated higher activity and light olefins selectivity.

Keywords: SAPO-34; MnAPSO-34; Molecular sieves; Mn incorporation; Si islands; Acidity; Ammonia adsorption; Chloromethane conversion; Light olefins

1. Introduction

In 1982, Wilson et al. reported for the first time the synthesis of aluminophosphate molecular sieves [1]. An interesting peculiarity of the electrically neutral AlPO-*n* materials is that Al and/or P can be replaced both by silicon to form SAPO-*n* [2,3], and by metal to form MeAPO-*n* or MeAPSO-*n* [4]. SAPOs have been reported as useful catalysts for a variety of chemical reactions [5–7]. MeAPOs and MeAPSOs were also proved to be excellent catalyst, such as MeAPO-11 and MeAPSO-11 in skeletal isomerization of *n*-butene [8,9] and MeAPSO-34 for higher ethylene production in MTO process [10,11].

* Corresponding author. Tel.: +32 81 724531; fax: +32 81 725414.
E-mail addresses: zml@dicp.ac.cn (Z. Liu), bao-lian.su@fundp.ac.be (B.-L. Su).
[1] Tel.: +86 411 84685510; fax: +86 411 84691570.

1387-1811/$ - see front matter © 2005 Elsevier Inc. All rights reserved.
doi:10.1016/j.micromeso.2005.10.042

Si incorporation into the framework of AlPO-*n* molecular sieves is the key to generate acid sites and the further metal incorporation can create additional modifications on the acidic properties and even give rise to redox catalytic properties of AlPO-*n* and SAPO-*n* [5–7,12]. In this field, a large series of works by Barthomeuf and co-workers generated a lot of knowledge and contributed to the important progress in understanding the topological structure of Si–P–Al framework, surface hydroxyl formation, thermal stability and acidic properties of SAPOs [13–22]. Her proposal concerning the Si island formation leading to Si substitution mechanisms was largely used to explain the acid sites formation in AlPO framework with Si incorporation [21–25]. For the metal-substituted molecular sieves, such as MeAPSO, although the acid site formation is also explained by the substitution mechanism [26], the framework polarization from metal incorporation is hard to prove because of the complication caused by multi-element substitution.

Isomorphous substitution of framework elements with Si and metal occurs during the synthesis of the molecular sieve. In this process, organic templates play an important role. Besides acting as the structure-directing agents, they also work as the charge compensator for the framework. When the neutral AlPO framework is negatively charged by Si^{4+} substitution for P^{5+} or bivalent metal Me^{2+} substitution for Al^{3+}, corresponding protonated template in channel will balance the framework negativity. With the template removal, proton will remain attached to framework oxygen, generating Brönsted acid sites. The study of the thermal effect upon template removal will give a lot of useful information not only on the choice of calcination condition, but also on understanding the nature of the framework properties. Minchev studied the thermal decomposition of organic template occluded in some SAPOs and MeAPO-5 molecular sieves, and attributed the difference of thermal effect to the difference of the channel structure and template–framework interaction [27,28]. Campelo and co-workers investigated the desorption and pyrolysis of different templates in N_2 atmosphere by means of high resolution mass spectrometry [29]. Barthomeuf et al. followed the template (TEAOH) departure from SAPO-34 with the technique of TGA and DTA [14]. However, the effect of metal incorporation on the template removal and corresponding acid sites generation in SAPO-34 and metal incorporated SAPO-34 have not been reported.

The present work studies the effect of Mn incorporation in SAPO-34 on the template removal and generation of Brönsted acid sites in MnAPSO-34. The chemical coordination environments of framework elements, P, Al and Si, of the synthesized SAPO-34 and MnAPSO-34 are investigated and compared by using ^{31}P, ^{27}Al and ^{29}Si MAS NMR. The template removal under diluted oxygen atmosphere is followed by means of TG–DTG–DSC coupled with mass spectrometry to determine the products of the template decomposition in different temperature ranges.

SAPO-34 and metal substituted SAPO-34 are famous catalysts for MTO process and their catalytic performance in methanol conversion have been intensively studied [10,11,30,31]. In our previous study, the metal substituted SAPO-34 showed excellent performance for light olefins production from methanol [32]. But for the chloromethane transformation to higher hydrocarbons [33–42], another potential and efficient way for natural gas utilization, the application of SAPO-34 is less studied. Kaiser gave one example with chloromethane as feedstock in his patent about the production of light olefins from aliphatic hetero compounds [43]. No report presents until now with metal-substituted SAPOs as the catalysts. So in the present work, beside the study mentioned above, SAPO-34 and MnAPSO-34, have been employed as the catalysts for chloromethane transformation to light olefins. The difference in catalytic performance caused by Mn incorporation was also investigated.

2. Experimental

2.1. Synthesis

SAPO-34 and MnAPSO-34 were prepared with hydrothermal method. Pseudoboehmite (PetroChina, China), orthophosphoric acid (85 wt%, LiaoningChem., China), colloidal silica (ShanghaiChem., China) and $Mn(CH_3COO)_2 \cdot 4H_2O$ (ShanghaiChem., China) were used as the sources of aluminum, phosphorus, silicon and manganese, respectively. Triethylamine (TEA) (XinxiChem., China) was used as the template. The synthesis of SAPO-34 and MnAPSO-34 followed the procedure reported in the literature [2–4]. The chemical composition of the starting gel was $1.0Al_2O_3$:$1.0P_2O_5$:$0.8SiO_2$:3.0TEA:$50H_2O$ for SAPO-34 and $1.0Al_2O_3$:$1.0P_2O_5$:$0.8SiO_2$:0.05MnO:3.0-TEA:$50H_2O$ for MnAPSO-34. The gels were sealed in the stainless-steel autoclave lined with polytetrafluoroethylene (PTFE) and the autoclave was heated at 200 °C for 24 h under autogeneous pressure. The products were filtrated, washed, and dried at 110 °C for 3 h.

2.2. Characterization of samples

The crystallinity and the phase purity of the as-synthesized samples were analyzed by powder X-ray diffraction (RIGAKU D/max-rb powder diffractometer) with CuKα radiation. The chemical composition of the samples was determined with Bruker SRS-3400 XRF spectrometer. Scanning electron microscope (SEM) images were obtained on a KYKY-1000 instrument operated at 25 kV. A JASCO V-550 unit was used for the diffuse reflectance UV–Vis measurement. ^{31}P, ^{27}Al and ^{29}Si MAS NMR spectra were recorded on a Bruker DRX-500 NMR spectrometer.

2.3. Template removal

The TG–DTG analysis in diluted oxygen (2% O_2 in Ar) and DSC thermal analysis was performed using

Perkin–Elmer Pyris-1 TGA and DTA 7. The sample was heated from 50 to 900 °C with a heating rate of 10 °C/min. The temperature-programmed decomposition products were analyzed in situ with Omnistar mass spectrometer (Balzers).

2.4. Ammonia adsorption evaluated with FT-IR

Self-supported SAPO-34 and MnAPSO-34 wafers (15 mg/cm^2) were first calcined in a Pyrex IR cell in oxygen at 450 °C for 10 h and then in vacuum for 4 h. After cooling to room temperature, the spectrum of the molecular sieve phase was recorded as a reference using a Fourier Transform Spectrum 2000 Spectrometer (Perkin–Elmer). The adsorption of known amounts of ammonia was then conducted on the wafers. After 0.5 h equilibration at room temperature, desorption experiments were carried out in the range from 200 to 400 °C for 0.5 h to evaluate the adsorption strength of ammonia in the samples.

2.5. Direct conversion of chloromethane

The catalytic tests of SAPO-34 and MnAPSO-34 were performed using a fixed bed reactor system at atmosphere pressure. Catalyst (0.62 g) was loaded into a quartz reactor with an inner diameter of 5 mm. The sample was pretreated in a flow of dry nitrogen at 500 °C for 1 h and then the temperature of reactor was adjusted to 450 °C and the atmosphere was replaced by nitrogen and chloromethane (the molar ratio of N_2/CH_3Cl was 1). The weight hourly space velocity (WHSV) was 3.17 h^{-1} for chloromethane. The reaction products were analyzed on-line by a Varian GC3800 gas chromatograph equipped with a FID detector and a PONA capillary column.

3. Results and discussion

3.1. Synthesis

3.1.1. Crystalline structure and morphological features by powder XRD and SEM

The XRD patterns of the as-synthesized SAPO-34 and MnAPSO-34 molecular sieves are shown in Fig. 1. The position and the intensity of the diffraction peaks of both samples are identical to those reported in the literature [1–4]. High intensity of XRD lines and absence of any baseline drift indicate high crystallinity without obvious impurity. Both samples have cubic morphology as shown in SEM photos (Fig. 2), noting that the size of MnAPSO-34 crystals is larger. The chemical composition of the calcined samples was determined by XRF and listed in Table 1.

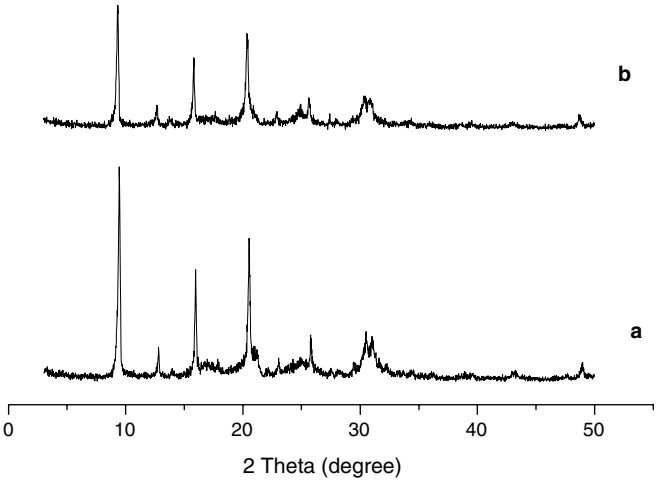

Fig. 1. XRD patterns of the as-synthesized samples: (a) SAPO-34 and (b) MnAPSO-34.

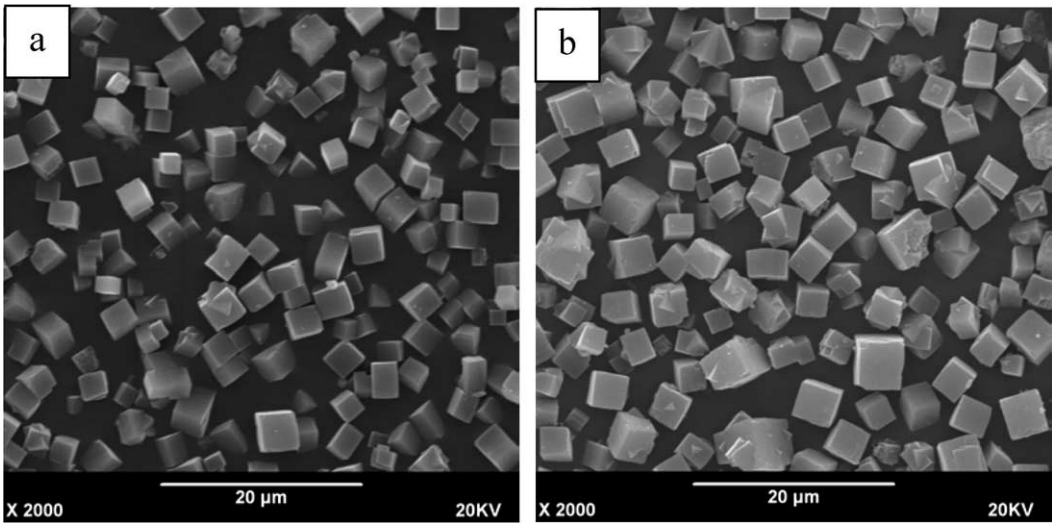

Fig. 2. SEM images of as-synthesized samples: (a) SAPO-34 and (b) MnAPSO-34.

Table 1
Molar composition of SAPO-34 and MnAPSO-34 molecular sieves

Sample	Molar composition	Mn content (wt%)
SAPO-34	$Al_{0.486}P_{0.409}Si_{0.105}O_2$	0
MnAPSO-34	$Al_{0.476}P_{0.411}Si_{0.093}Mn_{0.020}O_2$	1.8

3.1.2. Diffuse reflectance UV–Vis measurement

Fig. 3 shows diffuse reflectance UV–Vis spectra of the as-synthesized and calcined MnAPSO-34. The as-synthesized sample exhibits the band at about 255 nm, which has been attributed to tetrahedral Mn^{2+} species [10]. After calcination, the sample is pink in color and the absorption in violent region from Mn^{2+} species splits into two bands at 220 and 260 nm. A new absorption at around 500 nm appears in visible region, which indicates Mn^{3+} or Mn^{4+} species may be present after calcination. This absorbance may stem from the Mn species coordinated with either the defect sites or the framework of the aluminophosphate after the removal of template [44].

3.1.3. Chemical environment by ^{31}P, ^{27}Al and ^{29}Si MAS NMR spectra

Figs. 4 and 5 give the ^{31}P and ^{27}Al MAS NMR spectra, respectively, of the synthesized SAPO-34 (a) and MnAPSO-34 (b). The incorporation of Mn yields no apparent difference on the chemical shifts. The signal at −28.8 ppm in Fig. 4 should be attributed to the P(4Al) species in the framework. While the two signals at 39.2 and 7.7 ppm can be assigned to tetrahedrally coordinated and higher coordinated framework Al atoms respectively (Fig. 5). Previous reports have associated the signal at 7.7 ppm with pentacoordinated Al atoms formed by the additional coordination of one water to tetrahedrally coordinated Al species [45].

Fig. 6 shows the ^{29}Si MAS NMR spectra of SAPO-34 and MnAPSO-34. Five resonance signals appear in the

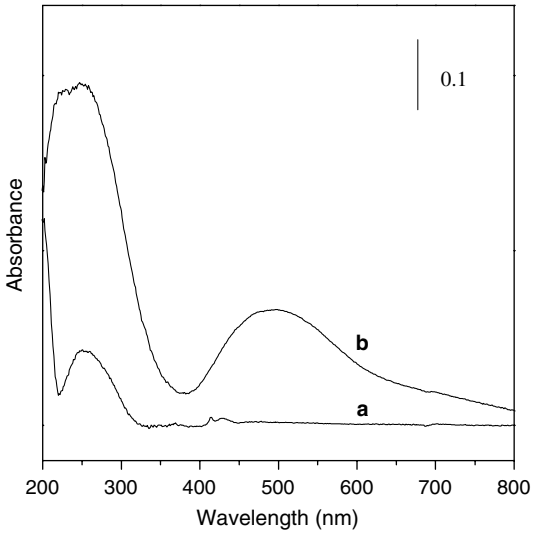

Fig. 3. DR UV–Vis spectra of the as-synthesized (a) and calcined MnAPSO-34 (b).

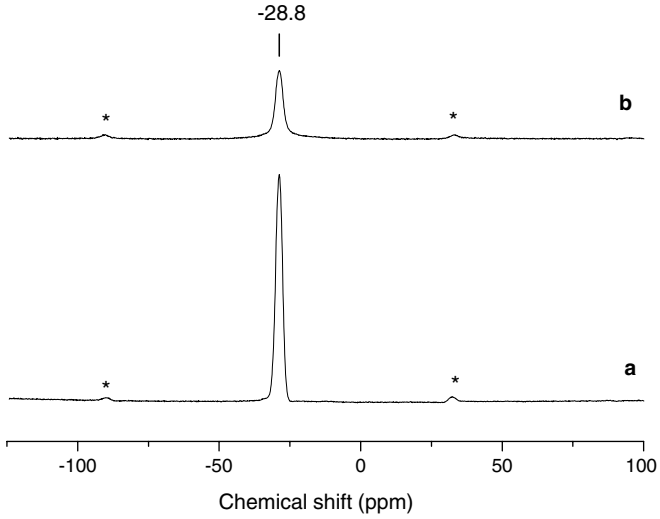

Fig. 4. ^{31}P MAS NMR spectra of SAPO-34 (a) and MnAPSO-34 (b).

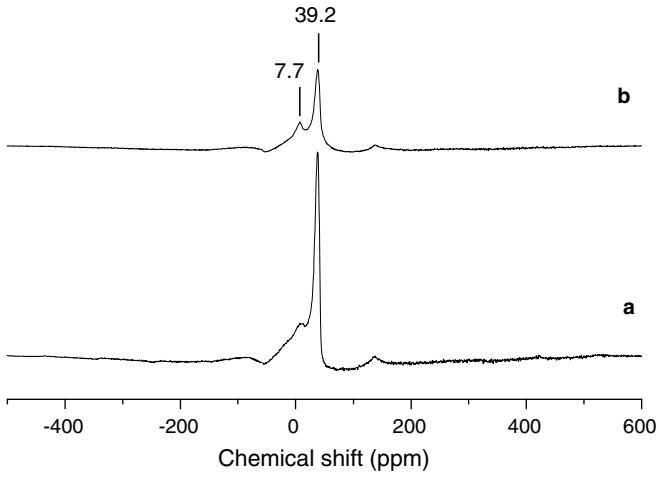

Fig. 5. ^{27}Al MAS NMR spectra of SAPO-34 (a) and MnAPSO-34 (b).

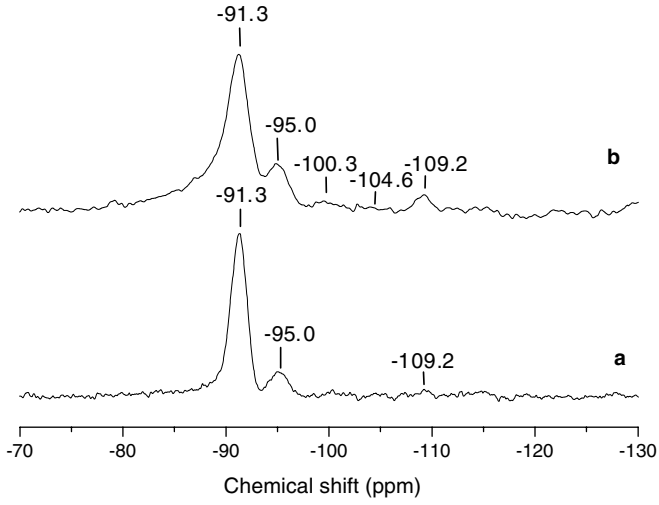

Fig. 6. ^{29}Si MAS NMR patterns of SAPO-34 (a) and MnAPSO-34 (b).

spectra. The signals with chemical shift of −91.3 and −95.0 ppm, stemming from the coordination states of Si(4Al) and Si(3Al) respectively, show relatively high intensity. The signals at −100.3, −104.8 and −109.2, originated from the coordination states of Si(2Al), Si(1Al) and Si(0Al) respectively, present relatively low intensity. In particular, those at −100.3 and −104.8 ppm were hardly visible. It is easy to see that, for the Mn-incorporated sample, the signal at −109.2 ppm is more prominent in intensity than that of SAPO-34.

It is known that Si atoms incorporate into the $AlPO_4$ framework by two substitution mechanisms: the first mechanism (SM2) is one Si substitution for one P to form Si(4Al) entities, which gives rise to negatively charged framework with relatively weak Brönsted acid sites. On the other hand, the double substitution of neighboring Al and P by two Si atoms to form Si(nAl) ($n = 3$–0) structures (SM3) leads to the formation of stronger Brönsted acid sites [21–25]. Usually, the coordination state of SAPO molecular sieve depends on the content of Si incorporation or the crystallization condition. For the two samples studied here, which were synthesized with the same condition and have very close amount of Si incorporation. The difference in their coordination state may result from the Mn incorporation.

Actually, from the ^{29}Si NMR spectra, in spite of roughly the very similar Si content in these two samples, Si(0Al) coordination of the MnSAPO-34 sample is more remarkable than that in SAPO-34. The prominent signal of Si(0Al) in MnAPSO-34 indicates that more Si islands may appear in the framework of MnAPSO-34. Because of the prohibition of the Si–O–P bonding in the framework, the corresponding Si–O–Al region will be generated at the border of the Si island [22–25,46]. Strong acid sites will thus form in this Si–Al region, with the properties similar to silicoaluminate zeolite.

3.2. Template removal

The results of TG–DTG–DSC in Table 2 and Fig. 7 show three weight losses (I, II and III) in the range of 50–900 °C for both two samples. The first weight loss (I) with endothermic effect in the range of 50–200 °C can be attributed to the water desorption from the samples. The very steep weight loss in the range of 200–400 °C and another relatively gradual weight loss in the range of 400–600 °C, both accompanied by an exothermic effect, correspond to the organic template TEA oxidation. The

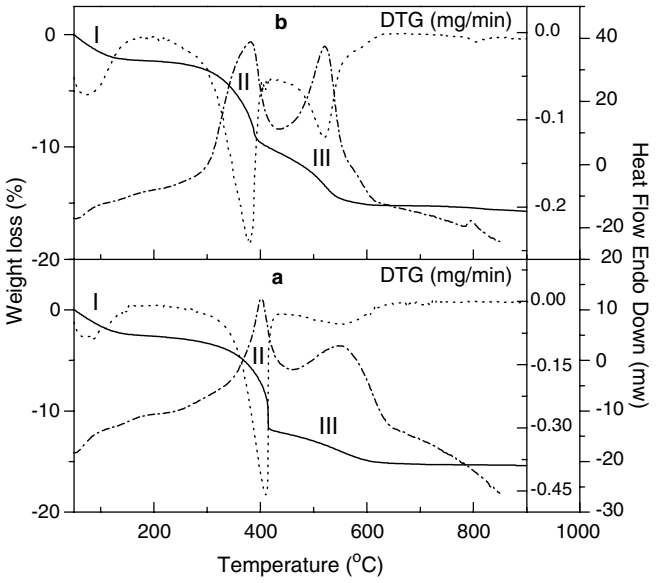

Fig. 7. TG–DTG–DSC of SAPO-34 (a) and MnAPSO-34 (b).

oxygen consumption in two temperature ranges has also been proved by MS result given in Fig. 8a. Previous study indicated that weight loss due to the template removal of some zeolites could occur in different temperature range [47–49]. For ZSM-5 zeolite with TEAOH as the synthesis template, two weight losses around 250 and 480 °C are assigned to the removal of TEAOH occluded in the zeolite and TEA^+ associated with $(Si–O–Al)^-$ group respectively [50]. In the present study, the presence of two weight losses related to template removal indicates that the template of TEA in the channel of SAPO-34 and MnAPSO-34 may have different chemical environment.

Comparing the two samples, even though the weight losses are in roughly the same temperature range, the proportion of weight loss in two template oxidation stages is different. For SAPO-34, the weight losses related to template removal are 74% and 26% for II and III, respectively. While for MnAPSO-34, weight loss at higher temperature range attained to 43%, with a more pronounced exothermic effect, indicating that the quantity of template in this environment is higher in MnAPSO-34.

Template decomposition can be related to the dimension of the channel system, the nature of the template and the template–framework interaction [27–29]. Minchev found that for some SAPOs with small porosity and one-dimensional channel system, it is difficult to completely remove

Table 2
Weight loss and thermal effect of the template removal

Stage	SAPO-34			MnAPSO-34		
	Temperature range (°C)	Weight loss (%)*	Thermal effect	Temperature range (°C)	Weight loss (%)*	Thermal effect
Stage I	50–200	–	Endothermic	50–200	–	Endothermic
Stage II	200–410	74	Exothermic	200–400	57	Exothermic
Stage III	410–600	26	Exothermic	400–600	43	Exothermic

* Only the weight loss (%) of stages II and III were calculated. The weight loss (%) of water is not included.

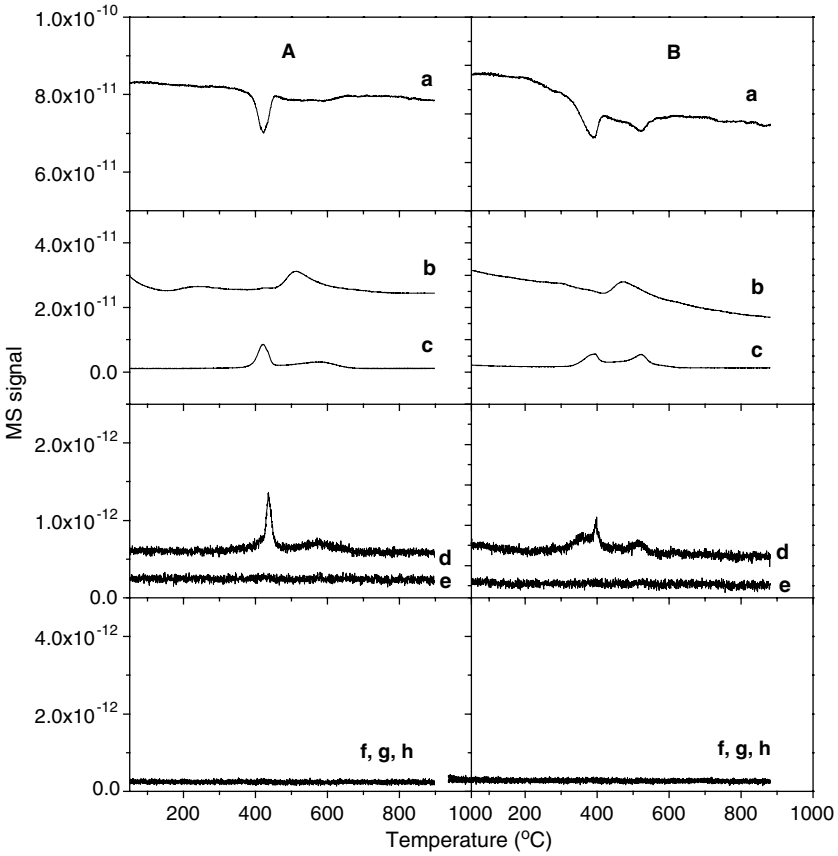

Fig. 8. Products determination of template decomposition of SAPO-34 (A) and MnAPSO-34 (B) with MS: (a) O_2, (b) H_2O, (c) CO_2, (d) NO, (e) NO_2, (f) $(C_2H_5)_3N$, (g) $(C_2H_5)_2NH$, (h) $(C_2H_5)NH_2$.

the template [27,28]. This was explained by the difficulty of oxygen diffusion or the carbon residue formation. He also found that SAPO synthesized with different templates showed different exothermic effect and weight loss. He attributed it to the template–framework interaction.

In our study, SAPO-34 and MnAPSO-34 possess the same structure of CHA, and are synthesized with the same template of TEA, but we still found some differences in thermal effect and weight loss during the template-calcination process. It is known that template acts as a charge compensator for the negatively charged lattice of zeolite, accompanying other cations in the channel [45,46]. For the substituted AlPOs, the isomorphous replacement of P^{5+} by Si^{4+} or Al^{3+} by bivalent metal ions Me^{2+} generates negatively charged framework. At the same time, no metal cations, such as Na^+, exist in the channel, so the charge of the framework will be balanced by negatively charged protonated template. After the removal of the template upon calcination, protons will be left for charge compensation and attached to framework oxygen atoms, so in this way, Brönsted acid sites form simultaneously. Usually, the protonated amine template is more difficult to remove than neutral template occluded in the channel, which is explained by the strong template–framework interaction between protonated template and negatively charged framework [45]. It was also found that, for zeolite, template removal is associated with OH generation and the template degradation temperature may predict the Brönsted acidity strength [51]. While for SAPOs and MeAPSOs, even though some research on their acidity has been done [26], the relationship between template removal and corresponding acid site formation caused by metal incorporation is still obscure. For the samples studied here, protonated template TEA, $(C_2H_5)_3NH^+$, acts as the charge compensator for the framework of Si or Si and Mn incorporated samples of SAPO-34 and MnAPSO-34. Considering the similar Si content of both samples, the difference of two samples in template–framework interaction may come from Mn incorporation. The different weight loss percentage and exothermal effect intensity in stages II and III observed in SAPO-34 and MnAPSO-34 suggest clearly the stronger template–framework interaction between template of TEA and MnAPSO-34 framework. After the removal of the template, more acidic sites with stronger acidity may accordingly generate.

The species from template decomposition were analyzed with in situ MS, the products from thermal template decomposition and oxygen consumption are shown in Fig. 8a–h. Three processes shown in Scheme 1 are expected to occur during the template removal: desorption, thermal cracking and oxide-decomposition, so all these possible products were tested with MS.

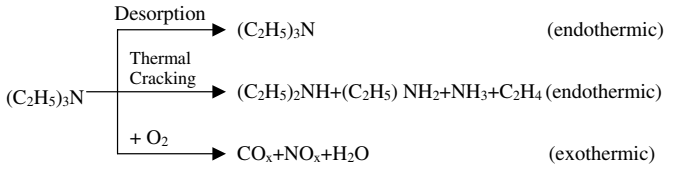

Scheme 1. Possible processes during the template removal.

From the MS result, CO_2($M/Z = 44$), NO ($M/Z = 30$) and H_2O ($M/Z = 18$) from template burning out with oxygen participation appear as the main products. Other possible products, such as methane, ethylene, ethane, ammonia, DEA (diethylamine) from thermal cracking during the calcination process or TEA from desorption just appear in trace amount. In Schnabel's work [52], when TEA is removed from AlPO-5 and SAPO-5 with oxygen participation, not only burning out, but also cracking and desorption took place. This may come from the difference of pore structure of SAPO-5 and SAPO-34. For SAPO-5 with one-dimension and 12-ring pore opening, the desorption of template molecule TEA or some cracking product, such as DEA is possible, but for SAPO-34 with eight-ring pore opening and cage structure, the template molecule desorption is more difficult.

During the template removal process for MnAPSO-34, oxygen consumption clearly appears in two temperature ranges of 200–420 and 420–600 °C, which indicate a two-stage oxygen-decomposition occurrence during the calcination. For SAPO-34, the first stage (200–420 °C) for O_2-consumption is more remarkable than the second temperature range of 420–600 °C. This corresponds to the weight loss, exothermal effect and product generation. In each range, CO_2, H_2O and NO are generated. This also proves the assumption that template molecule may exist in two kinds of environments, which results in their decomposition in different temperature range.

In Fig. 8, we can also find that for SAPO-34, the CO_2, NO generation and oxygen consumption appear mainly in the temperature range II, but for MnAPSO-34, decomposition in temperature range II and III appear roughly at the same level. The template decomposition in the higher temperature range usually indicates the stronger template–framework interaction. When TEA is removed in the high temperature range from MnAPASO-34, proton would be left in the channel as the charge compensator. Strong acidity would be generated.

3.3. Infrared study of adsorption of ammonia

Four peaks located at 3675, 3743, 3625 and 3598 cm^{-1} are observed from IR spectra of activated SAPO-34 and MnAPSO-34 (Fig. 9), representing four types of hydroxyl groups of the two samples. Two peaks at 3675 and 3743 cm^{-1} with low intensity are attributed to P–OH and Si–OH. Other two peaks at 3625 and 3598 cm^{-1} can be assigned to two types of Si(OH)Al groups differed in their localization. The bridged group with $\upsilon = 3598\ cm^{-1}$ were assumed to be localized in the hexagonal prism, forming an H-bond with adjacent oxygen atoms of the framework, while the isolated bridging OH groups pointing towards the center of the elliptical cages give the vibration frequency at 3625 cm^{-1} [13,14,53,54]. These two types of OH groups are considered to be the active sites for acid-catalyzing reactions [55,56].

Ammonia was used as probe to characterize the acidic property. After saturating the sample with ammonia at

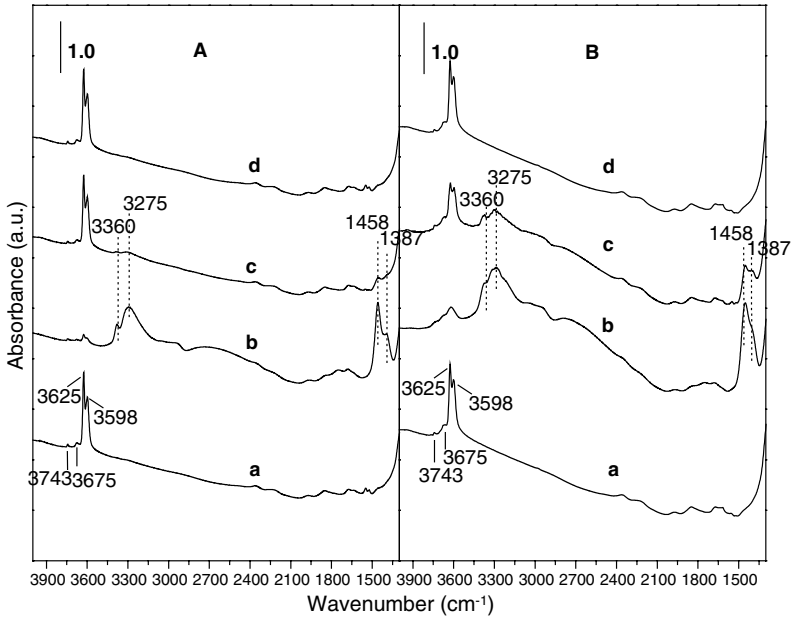

Fig. 9. Change in the infrared absorbance spectra of SAPO-34 (A) and MnAPSO-34 (B): activated sample (a) and of the adsorbed ammonia as a function of desorption temperature (°C) (b) 200, (c) 300 and (d) 400.

room temperature, an evacuation in vacuum is then performed at different temperatures during 0.5 h to remove the adsorbed ammonia. For two samples studied here, ammonia adsorption gives two absorbance peaks at 1458 and 1387 cm^{-1} in the range of 1600–1300 cm^{-1}, which may stem from the asymmetric and symmetric bending of H–N–H. The absorbance in these ranges is considered to be from the ammonium salts. In Barthomeuf's work, NH_3 adsorption on SAPO-34 induces the appearance of two bands at 1399 and 1454 cm^{-1}, which were attributed to ammonium ions [13]. In another study concerning ammonia adsorption on HZSM-5, the authors also assigned all the components in the 1350–1550 cm^{-1} to NH_4^+ vibration [57]. For the samples of SAPO-34 and MnAPSO-34 in the present study, the chemical adsorption of ammonia molecules upon the bridge hydroxyls generates ammonia ions, NH_4^+.

The adsorption of ammonia generates also two superimposed bands at 3275 and 3360 cm^{-1} in the zone of 2900–3500 cm^{-1}, which could be resulted from the interaction of ammonia with two types of hydroxyl groups at 3598 and 3625 cm^{-1}. It was previously reported that hydroxyl groups of zeolites or molecular sieves can be shifted to lower wavenumbers upon the interaction with a base molecule such as ammonia, pyridine or benzene [13,42,51,58,59]. The sharp decrease or disappearance of two bands at 3598 and 3625 cm^{-1} and simultaneous generation of two broad and superimposed bands at 3275 and 3360 cm^{-1}, respectively, indicate clearly that two broad bands at 3275 and 3360 cm^{-1} are indeed generated by the interaction of hydroxyls at 3598 and 3625 cm^{-1} with ammonia molecules and that these two hydroxyls are accessible to ammonia molecules.

It is observed that the intensity of the peaks in the zone of 1350–1550 and 2900–3500 cm^{-1} in Fig. 9c and d decreases with desorption temperature. In fact, for SAPO-34, over 300 °C, most of the NH_3 absorbance disappears in the spectra (Fig. 9A(c and d)) and the absorbance of two bridging hydroxyls is regenerated. For MnAPSO-34, complete desorption needs a higher temperature. From 100 to 300 °C, the peaks representing the adsorbed NH_3 decrease in intensity, but the complete desorption finishes until 400 °C. This difference in ammonia desorption implies a strength difference of acid-base interaction (OH–NH_3) of SAPO-34 and MnAPSO-34. The higher desorption temperature for MnAPSO-34 indicates its stronger acidity compared with that of SAPO-34.

3.4. Chloromethane conversion over SAPO-34 and MnAPSO-34

Catalytic testing of chloromethane transformation was carried out over SAPO-34 and MnAPSO-34 and the result of conversion and selectivity of the products are given in Figs. 10 and 11. The conversion evolution as a function of reaction time depicted in Fig. 10 shows that at the beginning of the transformation with reaction time of 5 min, the

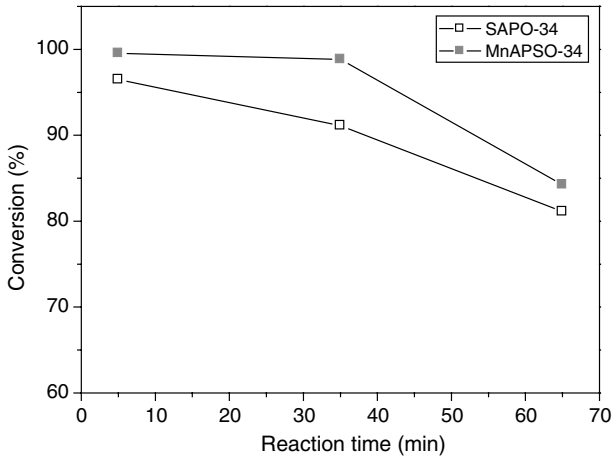

Fig. 10. Chloromethane conversion over SAPO-34 and MnAPSO-34.

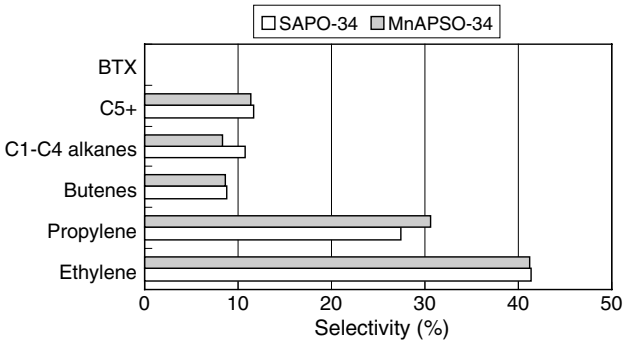

Fig. 11. Product distribution of chloromethane conversion over SAPO-34 and MnAPSO-34 molecular sieves.

conversion of chloromethane is 99.6% for MnAPSO-34 and 96.5% for SAPO-34, indicating the high initial activity of two samples. Prolonging the reaction time to 35 min, the chloromethane conversion over SAPO-34 slightly decreases to 91.1%, while MnAPSO-34 keeps its high activity. After a further increase in the reaction time to 65 min, some additional decrease observed, conversion over MnAPSO-34 (84.2%) is still higher than that of SAPO-34 (81.1%). This evolution of chloromethane conversion indicates that both catalysts lose part of the activity in chloromethane transformation, while MnAPSO-34 is more active. This may be from differences in their acidity, which has been proved by FT-IR.

Product distributions at reaction time of 65 min are detailed in Fig. 11. Among the products, for both catalysts, light alkenes, such as ethylene, propylene and butenes, are the main products (80% in total), indicating that SAPO-34 and MnAPSO-34 are very selective catalyst for the production of light alkenes from chloromethane. This result is quite different from zeolite catalyzed chloromethane transformation. In Taylor's work, chloromethane was mainly transferred to aromatics and paraffins [34,35]. In a very recent work, ethylene and propane appeared as the main products with cationic exchanged ZSM-5 [40,41]. This

interesting behavior, such as high selectivity for light olefins, similar to the excellent performance of SAPO-34 and MeAPSO-34 in MTO process [30,31], may stem from their eight-ring pore opening and medium acidity.

For the detailed olefins distribution (Fig. 11), roughly the same selectivity to ethylene and butenes is observed for the two samples, while propylene selectivity over MnAPSO-34 is higher than SAPO-34. Beside the light olefins, some other hydrocarbon products in small amount, such as light alkanes, around 10%, and products larger than C5+, about 8%, also appear. But for both samples, no aromatic products are obtained. SAPO-34 and MnAPSO-34's eight-membered ring pore openings sterically prohibit the desorption of aromatic products.

4. Conclusion

Mn incorporation into SAPO molecular sieves brings about the differences in Si coordination, template removal and acidity. Si(0Al) coordination state is more prominent for MnAPSO-34 than SAPO-34, which predicts the stronger acid site formation caused by Mn incorporation. When template is removed in oxygen atmosphere, because of the limitation of the pore structure, decomposition with the oxygen participation appears as the only way for template removal. The difference in weight loss, thermal effect and product generation reveals the different framework–template interaction between two samples. After template removal, stronger bridge hydroxyls are expected to form in the channel of MnAPSO-34. All the predictions about acidity difference were proved by FT-IR measurement of NH_3 adsorption, which is also in a good agreement with the conclusion of Si coordination states. Catalytic performance showed that SAPO-34 and MnAPSO-34 molecular sieves are very active and selective catalysts for the production of light olefins from chloromethane transformation. MnAPSO-34 shows higher chloromethane conversion and light olefins selectivity than SAPO-34, which is from the modification effect of Mn incorporation into the SAPO framework.

Acknowledgements

This work was realized in the frame of a European Inter Reg III program (France-Wallonie-Flandre—2.1.5). Y.-X. Wei thanks the University of Namur, for a Post-Doctor Scholarship.

References

[1] S.T. Wilson, B.M. Lok, C.A. Messina, E.R. Cannan, E.M. Flanigen, J. Am. Chem. Soc. 104 (1982) 1146.
[2] B.M. Lok, C.A. Messina, R.L. Patton, R.T. Gajek, T.R. Cannan, E.M. Flanigen, J. Am. Chem. Soc. 106 (1984) 6092.
[3] B.M. Lok, C.A. Messina, R.L. Patton, R.T. Gajek, T.R. Cannan, E.M. Flanigen, US Patent No. 4,440,871, 1984.
[4] B.M. Lok, B.K. Marcus, E.M. Flanigen, US Patent No. 4,686,092, 1987.
[5] I.M. Dahl, S. Kolboe, J. Catal. 149 (1994) 458.
[6] I.M. Dahl, S. Kolboe, J. Catal. 161 (1996) 304.
[7] J.M. Campelo, F. Lafont, J.M. Marinas, J. Chem. Soc., Faraday Trans. 91 (10) (1995) 1551.
[8] L.H. Gielgens, I.H.E. Veenstra, V. Ponec, M.J. Haanepen, J.H.C. van Hooff, Catal. Lett. 32 (1995) 195.
[9] A. Vieira, M.A. Tovar, C. Pfaff, B. Mendez, C.M. Lopez, F.J. Machado, J. Goldwasser, M.M.R. de Agudelo, J. Catal. 177 (1998) 60.
[10] N. Rajic, D. Stojakovic, S. Hocevar, V. Kaucic, Zeolites 13 (1993) 384.
[11] M. Kang, J. Mol. Catal.: Chem. 160 (2000) 437.
[12] Y. Wei, G. Wang, Z. Liu, P. Xie, Y. He, L. Xu, Catal. Lett. 91 (2003) 35.
[13] R. Vomscheid, M. Briend, M.J. Peltre, D. Barthomeuf, P.P. Man, J. Chem. Soc., Faraday Trans. 91 (1995) 3281.
[14] M. Briend, R. Vomscheid, M.J. Peltre, P.P. Man, D. Barthomeuf, J. Phys. Chem. 99 (1995) 8270.
[15] D. Barthomeuf, Zeolites 14 (1994) 394.
[16] M. Derewinski, M. Briend, M.J. Peltre, P.P. Man, D. Barthomeuf, J. Phys. Chem. 97 (1993) 13730.
[17] B.L. Su, D. Barthomeuf, Zeolites 13 (1993) 626.
[18] B.L. Su, A. Lamy, S. Dzwigaj, M. Briend, D. Barthomeuf, Appl. Catal. 75 (1991) 311.
[19] B.L. Su, D. Barthomeuf, Bull. Soc. Chim. Fr. 131 (1994) 730.
[20] M. Briend, A. Lamy, M.J. Peltre, P.P. Man, D. Barthomeuf, Zeolites 13 (1993) 201.
[21] P.P. Man, M. Briend, M.J. Peltre, A. Lamy, P. Beaunier, D. Barthomeuf, Zeolites 11 (1991) 563.
[22] R. Vomscheid, M. Briend, M.J. Peltre, P.P. Man, D. Barthomeuf, J. Phys. Chem. 98 (1994) 9614.
[23] R.B. Borade, A. Clearfield, J. Mol. Catal. 88 (1994) 249.
[24] A.M. Prakash, S. Unnikrishnan, J. Chem. Soc., Faraday Trans. 90 (1994) 2291.
[25] S. Ashtekar, S.V.V. Chilukuri, D.K. Chakrabarty, J. Phys. Chem. 98 (1994) 4878.
[26] D.B. Akolekar, J. Mol. Catal. A: Chem. 104 (1995) 95.
[27] C. Minchev, H. Weyda, V. Minkov, V. Penchev, H. Lechert, J. Thermal Anal. 37 (1991) 573.
[28] C. Minchev, V. Minkov, V. Penchev, H. Weyda, H. Lechert, J. Thermal Anal. 37 (1991) 171.
[29] J.M. Campelo, F. Lafont, J.M. Marinas, M. Ojeda, Rapid Commun. Mass Spectrom. 13 (1999) 521.
[30] C.D. Chang, Catal. Rev. Sci. Eng. 26 (3/4) (1984) 323.
[31] T. Inui, Stud. Surf. Sci. Catal. 105 (1997) 1441.
[32] L. Xu, Z. Liu, A. Du, Y. Wei, Z. Sun, Stud. Surf. Sci. Catal. 147 (2004) 445.
[33] G.A. Olah, B. Gupta, M. Farina, J.D. Felberg, W.M. Ip, A. Husain, R. Karpeles, K. Lammertsma, A.K. Melhotra, N.J. Trivedi, J. Am. Chem. Soc. 107 (1985) 7097.
[34] C.E. Taylor, R.P. Noceti, Stud. Surf. Sci. Catal. 36 (1988) 483.
[35] C.E. Taylor, R.R. Anderson, J.R. D'Este, R.P. Noceti, Stud. Surf. Sci. Catal. 130 (2000) 3633.
[36] P. Lersch, F. Bandermann, Appl. Catal. 75 (1991) 133.
[37] Y. Sun, S.M. Campbell, J.H. Lunsford, G.E. Lewis, D. Palke, L.M. Tau, J. Catal. 143 (1993) 32.
[38] D.K. Murray, J.-W. Chang, J.F. Haw, J. Am. Chem. Soc. 115 (1993) 4732.
[39] D.K. Murray, T. Howard, P.W. Goguen, T.R. Krawietz, J.F. Haw, J. Am. Chem. Soc. 116 (1994) 6354.
[40] D. Jaumain, B.L. Su, Stud. Surf. Sci. Catal. 130 (2000) 1607.
[41] D. Jaumain, B.L. Su, J. Mol. Catal. A: Chem. 197 (2003) 263.
[42] D. Jaumain, B.L. Su, Catal. Today 73 (2002) 187.
[43] S.W. Kaiser, US Patent No. 4,677,243, 1987.
[44] N.N. Tusar, G. Mali, I. Arcon, V. Kaucic, A. Ghanbari-Siahkali, J. Dwyer, Micropor. Mesopor. Mater. 55 (2002) 203.
[45] A. Buchholz, W. Wang, M. Xu, A. Arnold, M. Hunger, Micropor. Mesopor. Mater. 56 (2002) 267.

[46] G. Sastre, D.W. Lewis, C.R.A. Catlow, J. Phys. Chem. B 101 (1997) 5249.
[47] C.J. Jia, P. Massiani, D. Barthomeuf, J. Chem. Soc., Faraday Trans. 89 (1993) 3659.
[48] S.G. Hegde, R. Kumar, R.N. Bhat, P. Ratnasamy, Zeolite 9 (1989) 231.
[49] J. Perez-Pariente, J.A. Martens, P.A. Jacobs, Appl. Catal. 31 (1987) 35.
[50] L.M. Parker, D.M. Bibby, J.E. Patterson, Zeolite 4 (1984) 263.
[51] B.L. Su, V. Norberg, Zeolite 19 (1997) 65.
[52] K.-H. Schnabel, G. Finger, J. Kornatowski, E. Loffler, C. Peuler, W. Pilz, Micropor. Mater. 11 (1997) 293.
[53] S.A. Zubkov, L.M. Kustov, V.B. Kazansky, I. Girnus, R. Fricke, J. Chem. Soc., Faraday Trans. 87 (1991) 897.
[54] Y. Jeanvoine, J.G. Angyan, G. Kresse, J. Hafner, J. Phys. Chem. B 102 (1998) 5573.
[55] L. Smith, A.K. Cheetham, R.E. Morris, L. Marchese, J.M. Thomas, P.A. Wright, J. Chen, Science 271 (1996) 799.
[56] L. Smith, A.K. Cheetham, L. Marchese, J.M. Thomas, P.A. Wright, J. Chen, E. Gianotti, Catal. Lett. 41 (1996) 13.
[57] F. Lonyi, J. Valyon, Micropor. Mesopor. Mater. 47 (2001) 293.
[58] B.L. Su, D. Barthomeuf, J. Catal. 139 (1993) 81.
[59] B.L. Su, J.M. Manoli, C. Potvin, D. Barthomeuf, J. Chem. Soc. Faraday Trans. 89 (1993) 857.